

# Charmonium measurements at forward rapidity in Pb-Pb and p-Pb collisions with ALICE at LHC

Indranil Das<sup>1,a</sup> (on behalf of ALICE collaboration)

<sup>1</sup>*Institut de Physique Nucléaire d'Orsay*  
15 Rue Georges Clemenceau, 91406 Orsay

## Abstract.

Heavy-quark resonances, produced in high-energy heavy-ion collisions, are important observables for the study of quantum chromodynamics at extreme energy densities. In this paper, the nuclear modification factor and elliptic flow of  $J/\psi$  measured in the rapidity range ( $2.5 < y < 4$ ) of ALICE have been presented for Pb-Pb collisions at  $\sqrt{s_{NN}} = 2.76$  TeV. The recent ALICE results on the  $J/\psi$  nuclear modification factor in p-Pb collisions at  $\sqrt{s_{NN}} = 5.02$  TeV have also been discussed.

## 1 Motivation

A deconfined state of quarks and gluons can be produced in the ultra-relativistic heavy-ion collisions, which transform into hadrons when the temperature cools down. Lattice Quantum ChromoDynamics (QCD) calculations predict a phase transition from hadronic matter to a Quark Gluon Plasma (QGP) at high temperature and at extreme density [1, 2]. Since the heavy-quarks are produced at the early stage of the collisions, they are very important observables to understand the properties of QGP. Matsui and Satz [3] predicted that a charm quark-antiquark pair ( $c\bar{c}$ ) will experience the color screening in the deconfined interior of the QGP. Therefore, the production of  $J/\psi$  will be suppressed in heavy-ion collisions compared to the proton-proton collisions properly scaled, e.g. by the number of binary nucleon-nucleon or nuclear overlap function [4]. The higher excited states of charmonium, such as  $\chi_c$  and  $\psi(2S)$  decay to the  $J/\psi$  ground state with feed-down contribution of  $\sim 30\%$  and  $\sim 10\%$ , respectively [5]. Since the higher excited states are less bound compared to their ground state, the higher states will dissociate at lower temperature with respect to the dissociation temperature of ground state. This will lead to a sequential suppression pattern as suggested by Digal *et al.* [6, 7]. It was proposed that the copious production of  $c\bar{c}$  pairs can lead to charmonium production either by statistical production at the phase boundary [8], or through coalescence of charm quarks in the plasma [9]. In central Pb-Pb collisions at LHC energy the average number of  $c\bar{c}$  pairs increases substantially compared to that at RHIC energy, so that the statistical (re)generation mechanism could lead to an enhanced production compared to pp expectations [10]. Later, two transport models have been proposed which suggest partial regeneration [11, 12] from deconfined charm quarks in medium. These new models provide the combined effect of charmonium suppression in QGP (or hot medium) and regeneration from QGP, where charm quark thermalisation is taken into account.

---

<sup>a</sup>e-mail: indranil.das@cern.ch

Apart from the hot medium effects, there are (cold) nuclear matter effects which can influence charmonium production cross section in nucleus-nucleus (A-A) or proton-nucleus (p-A) collisions with respect to proton-proton (pp) collisions, such as,

- Nuclear shadowing : the Parton Distribution Functions (PDF) in nuclei are different from those in free protons and neutrons [13, 14].
- Saturation : at low  $x_{Bj}$  (Bjorken- $x$ ) momentum of hadrons, the nucleus is considered as a saturated gluonic system according to Color-Glass Condensate (CGC) theory. Therefore, the charmonium production in A-A can be different from those in pp collisions due to saturation [15].
- Energy loss : the coherent radiative energy loss of the partons in nuclear medium is different than that of pp collisions [16].
- $c\bar{c}$  break-up : due to the interaction with nuclear matter the  $c\bar{c}$  pair can break-up before the charmonium formation. However, this break-up can be neglected at LHC energy, because the interaction probability of  $c\bar{c}$  with nuclear medium is negligible due to the large Lorentz- $\gamma$  factor [17].

### 1.1 Nuclear modification factor

The (hot and cold) medium effects are measured in A-A and p-A collisions in terms of nuclear modification factor defined as  $R_{AA}^{J/\psi}$  and  $R_{pA}^{J/\psi}$ , respectively. Therefore in case of nucleus-nucleus collisions,

$$R_{AA}^{J/\psi} = \frac{Y_{AA}^{J/\psi}}{\langle T_{AA} \rangle \sigma_{pp}^{J/\psi}} \quad (1)$$

where  $Y_{AA}^{J/\psi}$  is the inclusive  $J/\psi$  yield in A-A collisions,  $\langle T_{AA} \rangle$  is nuclear overlap factor calculated using the Glauber model and  $\sigma_{pp}^{J/\psi}$  is  $J/\psi$  production cross section in pp collisions. The measured inclusive  $J/\psi$  is an admixture of direct  $J/\psi$  production, feed-down from higher  $\chi_c$ ,  $\psi(2S)$  states and B hadron decay to  $J/\psi$ .

In p-A collisions the medium effects are measured as  $R_{pA}^{J/\psi}$ ,

$$R_{pA}^{J/\psi} = \frac{Y_{pA}^{J/\psi}}{\langle T_{pA} \rangle \sigma_{pp}^{J/\psi}}$$

or as the ratio of the forward to the backward yields ( $R_{FB}$ ),

$$R_{FB} = \frac{Y_{pA}^{Forward}}{Y_{pA}^{Backward}} \quad (2)$$

where the notations represent the same observables as of Eqn. 1, but for p-A collisions.

### 1.2 Elliptic flow

The collective spatial expansion of the fireball created in heavy-ion collisions is termed as Flow. If a non-negligible regeneration effect is present then the  $J/\psi$ s generated from thermalised medium will carry the signature of collective spatial expansion of the medium. Hence, models predict that the regenerated  $J/\psi$ s will exhibit flow [11, 12]. This is an important observation since the STAR

measurement of the elliptic flow of  $J/\psi$  is found to be consistent with zero within errors in Au-Au collisions at  $\sqrt{s_{NN}} = 200$  GeV [18].

In experiment the flow is measured using the azimuthal particle distribution. The second coefficient of the Fourier expansion ( $v_2$ ) describing the azimuthal distribution with respect to the reaction plane is called elliptic flow, where the reaction plane is defined by the beam axis and the impact parameter vector of the colliding nuclei. In the present analysis the  $v_2$  of inclusive  $J/\psi$  is obtained by determining  $v_2 = \langle \cos 2(\phi - \Psi) \rangle$  versus invariant mass ( $m_{\mu\mu}$ ) [19], where  $\phi$  is the dimuon azimuthal angle and  $\Psi$  is the angle of the reaction plane. In this method,  $v_2$  of the oppositely signed (OS) dimuons is calculated as a function of  $m_{\mu\mu}$  and then the resulting  $v_2(m_{\mu\mu})$  distribution is fitted using:

$$v_2(m_{\mu\mu}) = v_2^{\text{sig}} \alpha(m_{\mu\mu}) + v_2^{\text{bkg}}(m_{\mu\mu}) [1 - \alpha(m_{\mu\mu})], \quad (3)$$

where  $v_2^{\text{sig}}$  and  $v_2^{\text{bkg}}$  correspond to the  $v_2$  of the  $J/\psi$  signal and of the background, respectively. Here,  $\alpha(m_{\mu\mu}) = S/(S + B)$  is the ratio of the signal over the sum of the signal plus background in a given  $m_{\mu\mu}$  bin. It is extracted from fits to the OS invariant mass distribution for given  $p_T$  range and centrality class. Consistent  $v_2$  values are obtained using an alternative method [20] in which the  $J/\psi$  raw yield is extracted as described before, in bins of  $(\phi - \Psi)$ . The  $v_2$  values are evaluated using a fit to the data with the function  $\frac{dN}{d(\phi - \Psi)} = A[1 + 2v_2 \cos 2(\phi - \Psi)]$ , where  $A$  is a normalization constant. A similar method is applied to extract the uncorrected  $p_T$  ( $\langle p_T \rangle^{\text{uncorr}}$  not corrected for detector acceptance and efficiency) of  $J/\psi$ .

## 2 Experimental setup and analysis methods

ALICE is a general purpose experiment whose detectors identify and measure hadrons, electrons, photons and muons produced in pp, p-Pb and Pb-Pb collisions at the LHC of CERN [21]. Charmonia are independently measured in two detector systems of ALICE, at midrapidity ( $-0.9 < y < 0.9$ ) via the electron channel and at forward rapidity ( $2.5 < y < 4.0$ ) using the muon decay channel. In both cases the ALICE measures  $J/\psi$  down to  $p_T = 0$ . In the present analysis the inclusive  $J/\psi$  at forward rapidity is measured in the Muon Spectrometer (MS). It consists of 10 cathode pad chambers (tracking detectors) and 4 resistive plate chambers (trigger detectors) with a 1.2 meter thick iron wall in between the last tracking chamber and first trigger chamber. The fifth and sixth tracking detectors are placed inside a dipole magnet of 3 Tm field integral. In addition, a front absorber ( $10\lambda$ ) between the collision vertex and first tracking detector stops the low momentum pions and kaons before they decay into muon.

Two other detectors have been used in this analysis which are VZERO counters and silicon pixel detector (SPD). All of these detectors including MS have full azimuthal coverage. The VZERO scintillator detector is made of two sets of arrays known as VZERO-A and VZERO-C on each side of the interaction point covering  $2.8 < \eta < 5.1$  and  $-3.7 < \eta < -1.7$ , respectively. Apart from the minimum bias trigger information, the amplitude of the VZERO-A signal is used to estimate the second harmonic event plane ( $\Psi$ ) of Pb-Pb collisions in flow analysis of  $J/\psi$ . The SPD, used to determine the location of the interaction point, consists of two cylindrical layers covering  $|\eta| \leq 2.0$  and  $|\eta| \leq 1.4$  for the inner and outer layers, respectively.

Two data taking periods have been utilised, one for Pb-Pb colliding beams at  $\sqrt{s_{NN}} = 2.76$  TeV with integrated luminosity  $\mathcal{L}_{\text{int}} \approx 70 \mu\text{b}^{-1}$  and another for p-Pb collisions at  $\sqrt{s_{NN}} = 5.02$  TeV with two beam configurations,

- p-Pb : proton along the upstream of MS ( $2.03 < y_{\text{cms}} < 3.53$ ) with  $\mathcal{L}_{\text{int}} \approx 5.03 \text{ nb}^{-1}$
- Pb-p : Pb along the upstream of MS ( $-4.46 < y_{\text{cms}} < -2.96$ ) with  $\mathcal{L}_{\text{int}} \approx 5.81 \text{ nb}^{-1}$

In case of p-Pb/Pb-p collisions, the positive rapidities refer to the direction of the proton beam. The analysis have been carried out on events where oppositely charged muon tracks have been fired in the muon trigger detector on top of minimum bias (MB) trigger, where MB trigger is a coincidence trigger of VZERO-A and VZERO-C signals. In offline analysis the information of various ALICE detectors are collected to select events which comes from proper interaction vertex. This is based on the checks of a) proper interaction trigger, b) correct event type, c) correct online trigger conditions and d) not from beam-gas collisions and not from debunched beam [22]. Some analysis specific cuts, such as the centrality estimation using VZERO (for Pb-Pb collisions) and limit on z-position of collision vertex  $|z_{\text{vertex}}| < 10$  cm (for elliptic flow study) have been used when necessary. The oppositely charged muon tracks are selected so that each track in the tracking detector matches with a trigger tracklet and each track is within  $-4.0 < \eta_{\mu} < -2.5$  whereas the combined rapidity of dimuon pair is  $2.5 < y_{\mu\mu} < 4.0$ . In addition, a cut on the track radial position on absorber end  $17.6 < R_{\text{abs}} < 89$  cm is applied for further filtering of dimuon spectra. Then dimuon mass spectrum is fitted with signal and background functions to extract the number of  $J/\psi$  for given analysis cuts.

## 3 Results

### 3.1 Charmonium measurements in Pb-Pb collisions

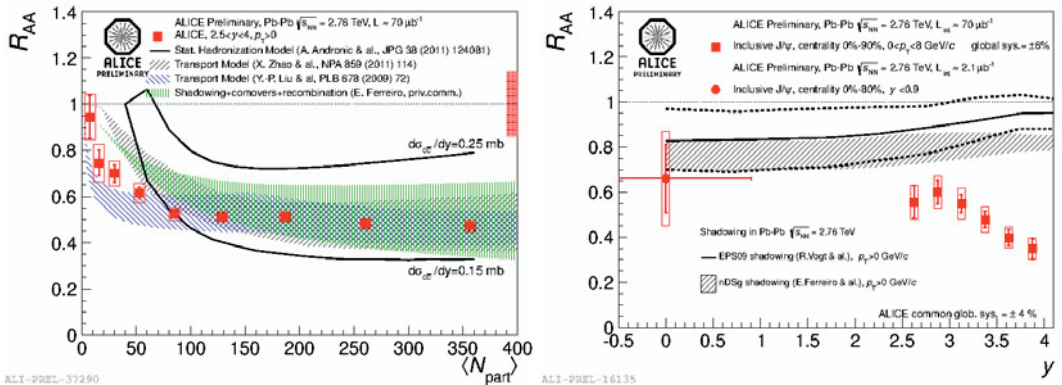


**Figure 1.** Left : the  $R_{AA}$  measurement of inclusive  $J/\psi$  as functions of number of participating nucleons. Right : the inclusive  $J/\psi$   $R_{AA}$  vs rapidity. The boxes around the points represent the uncorrelated systematic uncertainties, where as the filled box close to unit  $R_{AA}$  shows global systematic uncertainties [23].

### Nuclear modification factor

The nuclear modification factor of the inclusive  $J/\psi$  is measured in the forward rapidity region for the Pb-Pb collisions at  $\sqrt{s_{NN}} = 2.76$  TeV [23–25]. The inclusive  $R_{AA}$  integrated over centrality,  $p_T$  and  $y$  is  $0.497 \pm 0.006(\text{stat}) \pm 0.078(\text{syst})$  [24]. In the left panel of Fig. 1, the  $R_{AA}$  is plotted as function of number of participant nucleons ( $\langle N_{\text{part}} \rangle$ ). The data show no centrality dependence for  $\langle N_{\text{part}} \rangle$  above 70. It is interesting to note that the statistical regeneration and transport models are in good agreement with data. In the right side of Fig. 1, the variation of  $R_{AA}$  is shown with rapidity. Although the theoretical models of nuclear shadowing can describe the ALICE data in midrapidity domain, it is not describing the experimental data in the forward rapidity. The regeneration mechanism is expected to play a dominant role in central collisions compared to peripheral collisions since the number of

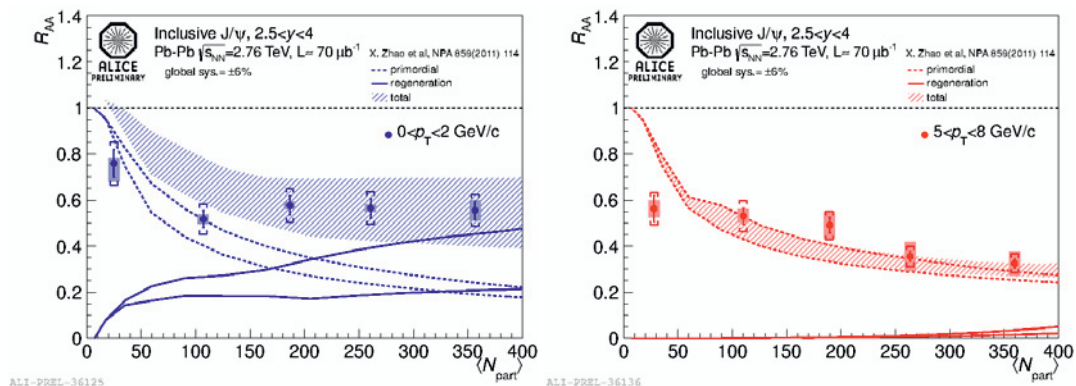


**Figure 2.** The inclusive  $J/\psi$   $R_{AA}$  measurement vs the number of participating nucleons for  $0 < p_T < 2$  GeV/c (left) and  $5 < p_T < 8$  GeV/c (right). The uncorrelated and partially correlated systematic uncertainties are shown as boxes and brackets, respectively [25].

$c\bar{c}$  created in central collisions is higher than peripheral collisions. Furthermore, the particles created from the regenerated medium are supposed to carry less momentum than the one created from hard collisions as the regeneration occurs at later stage of heavy-ion collisions compared to initial hard scatterings. Therefore the  $R_{AA}$  is separately plotted for two  $p_T$  intervals in Fig. 2. While comparing the data with the transport model predictions, it becomes evident that the regeneration contribution becomes maximum at low  $p_T$  in most central collisions.

### Elliptic flow

Footprints of regeneration may also appear in the inclusive  $J/\psi$  elliptic flow results. If the  $J/\psi$  from

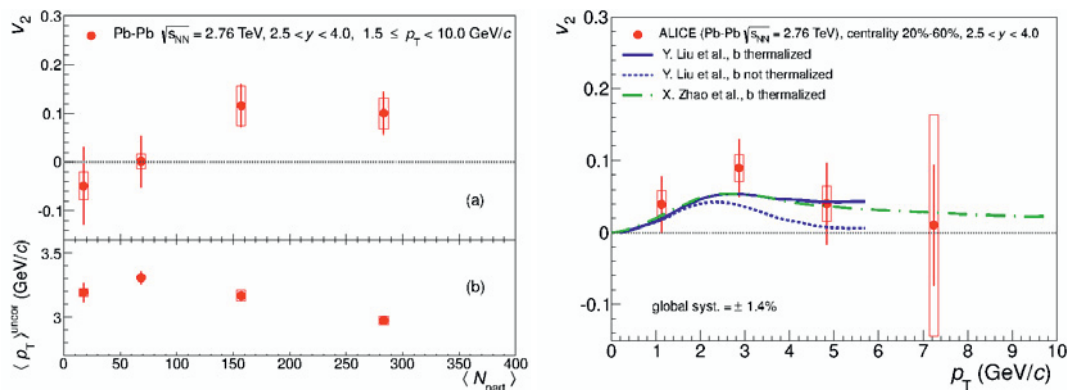


**Figure 3.** Left : (a) the  $v_2$  measurement of inclusive  $J/\psi$  as functions of number of participating nucleons, (b) dependence of  $\langle p_T \rangle^{uncorr}$  on centrality. Right :  $v_2$  vs uncorrected  $p_T$  [23].

the regenerated charm quarks of QGP, has non-negligible contribution to the total number of  $J/\psi$ , it will be manifested as the elliptical flow of  $J/\psi$ . In the left panel of Fig. 3(a) the inclusive elliptic flow of  $J/\psi$  is found non-zero for semi-central Pb-Pb collisions at  $\sqrt{s_{NN}} = 2.76$  TeV [26–28]. Since the

$v_2$  is found to be dependent on centrality and  $\langle p_T \rangle^{\text{uncorr}}$ , the dependence of  $\langle p_T \rangle^{\text{uncorr}}$  on centrality is plotted in the left panel of Fig. 3(b). The right plot of Fig. 3 shows  $v_2$  variation as function of uncorrected  $p_T$  of  $J/\psi$ . The largest measured  $v_2$  value is  $0.116 \pm 0.046(\text{stat.}) \pm 0.029(\text{syst.})$  in the transverse momentum range  $2 < p_T < 4$  GeV/c for semi-central Pb-Pb collisions [28]. Once again the same transport models which explain the  $R_{AA}$  results are able to describe the experimental points with 50% regeneration from the deconfined medium. The LHCb collaboration has measured a substantial contribution of B hadron decay to  $J/\psi$  for pp collisions in forward rapidity [29, 30]. Therefore if the b quarks are thermalised, it will be transferred to B hadron and the flow of B hadron will be measured as the flow of  $J/\psi$ . Both the contributions of thermalised and non-thermalised b quarks have been calculated from models and both of them qualitatively describe the  $p_T$  dependence of  $J/\psi$  elliptic flow.

### 3.2 Charmonium measurements in p-Pb collisions

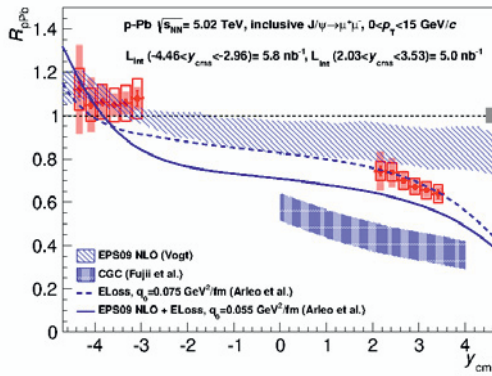


**Figure 4.** The  $R_{pA}$  measurement of  $J/\psi$  as functions of rapidity [23].

In order to understand the contribution of the cold nuclear matter effects, ALICE have measured the charmonium production for p-Pb collisions at  $\sqrt{s_{NN}} = 5.02$  TeV [31]. Since the experimental cross section of  $J/\psi$   $\sigma_{pp}^{J/\psi}$  is not available for  $\sqrt{s} = 5.02$  TeV, the extrapolated results from lower energy measurement at  $\sqrt{s} = 2.76$  TeV [32] and  $\sqrt{s} = 7$  TeV have been used for the calculation of  $R_{pA}^{J/\psi}$ . The nuclear modification factor as calculated for two beam configurations are [31],

$$R_{pPb} = 0.70 \pm 0.01(\text{stat.}) \pm 0.04(\text{syst.uncorr.}) \pm 0.03(\text{syst.part.corr.}) \pm 0.03(\text{syst.corr.})$$

$$R_{pPb} = 1.08 \pm 0.01(\text{stat.}) \pm 0.08(\text{syst.uncorr.}) \pm 0.07(\text{syst.part.corr.}) \pm 0.04(\text{syst.corr.})$$

In Fig. 4 the  $R_{pA}^{J/\psi}$  has been shown for smaller bins of rapidity. It can be inferred from both plots that the theoretical calculation of coherent parton energy loss and shadowing using EPS09 parameterisation are in close agreement with the experimental points whereas the CGC model is away from the data.

The ratio of forward to backward yields (Eqn. 2) have been found to be  $R_{FB} = 0.60 \pm 0.01(\text{stat.}) \pm 0.06(\text{syst.})$  for overlapping rapidity region of  $2.96 < |y_{cms}| < 3.53$ . On the left side of Fig. 5 the variation of  $R_{FB}$  is shown as a function of  $y_{cms}$ , whereas on the right,  $R_{FB}$  is plotted as a function of  $p_T$  of  $J/\psi$ . When compared to the theoretical models, the shadowing and energy loss predictions seem to reproduce part of the data for both plots.

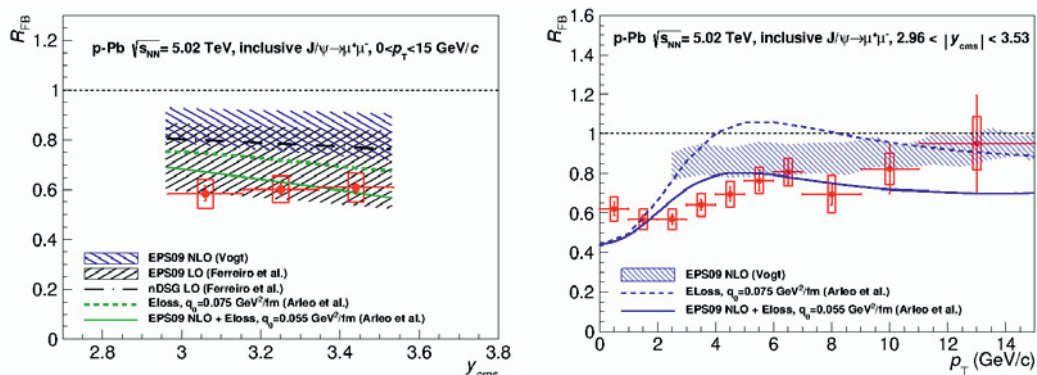


**Figure 5.** The  $R_{FB}$  measurement of inclusive  $J/\psi$  as functions of rapidity (left) and  $p_T$  (right) [23].

## 4 Conclusions

ALICE has carried out the measurement of charmonium in pp, p-Pb and Pb-Pb collisions. Present results at forward rapidity show a saturation in the suppression from semi-central to central collisions of  $R_{AA}$  plot. Further support for regeneration can be deduced from the  $p_T$  dependence of the nuclear modification factor. In addition, flow results also seem to be consistent with the regeneration model. Apart from the hot medium effects the cold nuclear matter effects, have been also studied. Although the Pb-Pb and p-Pb collisions have been performed at different energies, a first approximation of  $R_{PbPb}$  from the p-Pb collisions ( $R_{pPb} \times R_{Ppb}$ ) gives  $0.76 \pm 0.07(\text{stat}) \pm 0.10(\text{syst})$  which is still higher than what was observed in Pb-Pb collisions :  $R_{PbPb} = 0.497 \pm 0.006(\text{stat}) \pm 0.078(\text{syst})$ . This crude estimation suggests that the suppression in Pb-Pb collisions can not be only due to cold nuclear matter effects.

## References

- [1] N. Cabibbo and G. Parisi, Phys. Lett. B **59**, 67 (1975)
- [2] J. C. Collins and M. J. Perry, Phys. Rev. Lett. **34**, 1353 (1975)
- [3] T. Matsui and H. Satz, Phys. Lett. B **178**, 416 (1986)
- [4] The ALICE Collaboration, arXiv:1301.4361
- [5] N. Brambilla *et al.*, Eur. Phys. J. C **71**, 1534 (2011)
- [6] S. Digal, P. Petreczky and H. Satz, Phys. Rev. D **64**, 094015 (2001)
- [7] S. Digal, H. Satz and R. Vogt, Phys. Rev. D **85**, 034906 (2012)
- [8] P. Braun-Munzinger and J. Stachel, Phys. Lett. B **490**, 196 (2000)
- [9] R. L. Thews, M. Schroedter and J. Rafelski, Phys. Rev. C **63**, 054905 (2001)
- [10] A. Andronic, P. Braun-Munzinger, K. Redlich and J. Stachel, Nucl. Phys. A **789**, 334 (2007)
- [11] X. Zhao and R. Rapp, Nucl. Phys. A **859**, 114 (2011)
- [12] Y. Liu, Z. Qu, N. Xu, and P. Zhuang, Phys. Lett. B **678**, 72 (2009)
- [13] J. J. Aubert *et al.* (EMC Collaboration), Phys. Lett. B **123**, 275 (1983)
- [14] K. J. Eskola, H. Paukkunen and C. A. Salgado, JHEP **04**, 065 (2009)
- [15] D. Kharzeev and K. Tuchin, Nucl. Phys. A **770**, 40 (2006)
- [16] F. Arleo and S. Peigné, Phys. Rev. Lett. **109**, 122301 (2012)

- [17] R. Vogt, Nucl. Phys. A **700**, 539 (2002)
- [18] The STAR Collaboration, Phys. Rev. Lett. **111**, 052301 (2013)
- [19] N. Borghini and J. Y. Ollitrault, Phys. Rev. C **70**, 064905 (2004)
- [20] A. M. Poskanzer and S. A. Voloshin, Phys. Rev. C **58**, 1671 (1998)
- [21] The ALICE Collaboration, JINST **3**, S08002 (2008)
- [22] The ALICE Collaboration, Phys. Rev. Lett. **109**, 252302 (2012)
- [23] The ALICE Collaboration, Phys. Rev. Lett. **109**, 072301 (2012)
- [24] The ALICE Collaboration, Nucl. Phys. A **904-905**, 595c (2013)
- [25] The ALICE Collaboration, Nucl. Phys. A **904-905**, 202c (2013)
- [26] The ALICE Collaboration, Nucl. Phys. A **910-911**, 235 (2013)
- [27] The ALICE Collaboration, Nucl. Phys. A **904-905**, 673c (2013)
- [28] The ALICE Collaboration, arXiv:1303.5880
- [29] The LHCb Collaboration, JHEP **02**, 041 (2009)
- [30] The LHCb Collaboration, Eur. Phys. J. C **71**, 1645 (2011)
- [31] The ALICE Collaboration, arXiv:1308.6726
- [32] The ALICE Collaboration, Phys. Lett. B **718**, 295 (2012)